Sirtuin-1 (SIRT1) stimulates growth-plate chondrogenesis by attenuating the PERK–eIF-2α–CHOP pathway in the unfolded protein response

Received for publication, August 1, 2017, and in revised form, March 21, 2018 Published, Papers in Press, April 13, 2018, DOI 10.1074/jbc.M117.809822

Xiaomin Kang[‡1], Wei Yang[‡1], Ruiqi Wang[‡], Tianping Xie[‡], Huixia Li[§], Dongxu Feng[‡¶], Xinxin Jin[‡], Hongzhi Sun[§2], and Shufang Wu[‡3]

From the [‡]Center for Translational Medicine, the First Affiliated Hospital of Xi'an Jiaotong University School of Medicine, Xi'an, Shaanxi 710061, China, the [§]Key Laboratory of Environment and Genes Related to Diseases, Ministry of Education, Medical School of Xi'an Jiaotong University, Xi'an, Shaanxi 710061, China, and the [¶]Hong Hui Hospital, Xi'an Jiaotong University School of Medicine, Xi'an, Shaanxi 710054, China

Edited by Amanda J. Fosang

The NAD$^+$-dependent deacetylase sirtuin-1 (SIRT1) has emerged as an important regulator of chondrogenesis and cartilage homeostasis, processes that are important for physiological skeletal growth and that are dysregulated in osteoarthritis. However, the functional role and underlying mechanism by which SIRT1 regulates chondrogenesis remain unclear. Using cultured rat metatarsal bones and chondrocytes isolated from rat metatarsal rudiments, here we studied the effects of the SIRT1 inhibitor EX527 or of SIRT1 siRNA on chondrocyte proliferation, hypertrophy, and apoptosis. We show that EX527 or SIRT1 siRNA inhibits chondrocyte proliferation and hypertrophy and induces apoptosis. We also observed that SIRT1 inhibition mainly induces the PERK–eIF-2α–CHOP axis of the endoplasmic reticulum (ER) stress response in growth-plate chondrocytes. Of note, EX527- or SIRT1 siRNA–mediated inhibition of metatarsal growth and growth-plate chondrogenesis were partly neutralized by phenylbutyric acid, a chemical chaperone that attenuates ER stress. Moreover, EX527-mediated impairment of chondrocyte function (*i.e.* of chondrocyte proliferation, hypertrophy, and apoptosis) was partly reversed in CHOP$^{-/-}$ cells. We also present evidence that SIRT1 physically interacts with and deacetylates PERK. Collectively, our findings indicate that SIRT1 deacetylates PERK and attenuates the PERK–eIF-2α–CHOP axis of the unfolded protein response pathway and thereby promotes growth-plate chondrogenesis and longitudinal bone growth.

This work was supported by National Natural Science Foundation of China Program Grants 81672221, 81472038, 81370899, and 81170741; National Excellent Young Scientist Program Grant 81222026; and Ministry of Education of China New Century Excellent Talents Grant NCET-11-0437. The authors declare that they have no conflicts of interest with the contents of this article.

This article contains Figs. S1–S6.

[1] Both authors contributed equally to this work.

[2] To whom correspondence may be addressed: Key Laboratory of Environment and Genes Related to Diseases, Ministry of Education, Medical School of Xi'an Jiaotong University, 76 West Yanta Rd., Xi'an, Shaanxi 710061, China. Tel.: 86-13186063965; E-mail: sunhongzhi@mail.xjtu.edu.cn.

[3] To whom correspondence may be addressed: Center for Translational Medicine, First Affiliated Hospital of Xi'an Jiaotong University School of Medicine, 277 West Yanta Rd., Xi'an, Shaanxi 710061, China. Tel.: 86-18991232564; E-mail: shufangw@hotmail.com.

Sirtuin-1 (SIRT1),[4] a NAD$^+$-dependent histone deacetylase, exerts a variety of biological function through the deacetylation of not only lysine residues in histone (1) but also nonhistone proteins, such as p53 (2), forkhead family proteins (3), and p65/RelA subunit of NF-κB (NF-κB) (4). Through deacetylation, SIRT1 is involved in a variety of biological processes such as stress responses, DNA repair, and inflammation (5, 6) and plays a crucial part in regulating cell differentiation, proliferation, survival, and organism longevity (7, 8).

Previous evidence indicates that SIRT1 exerts a regulatory role in cartilage homeostasis. In human chondrocytes derived from osteoarthritis (OA) patients, overexpressing or activating SIRT1 enhances the expression of cartilage anabolic genes such as Col2a1 and aggrecan (9). It has also been shown that SIRT1 protects chondrocytes from radiation-induced senescence (10) and inhibits human chondrocyte apoptosis *in vitro* (11, 12). Furthermore, inhibition of SIRT1 in human chondrocytes leads to OA-like gene expression changes (13), and cartilage-specific SIRT1 knockout mice show accelerated OA progression (14), suggesting that SIRT1 has a protective role in articular cartilage. With respect to SIRT1 effects on growth-plate chondrocytes, previous studies indicate that SIRT1-null mice and mice with a SIRT1 point mutation exhibit significant reduction in body size (15, 16), implicating that SIRT1 involved in growth-plate chondrogenesis and, in turn, longitudinal bone growth.

In mammals, the long bone is mainly formed via endochondral ossification, which occurs at the epiphyseal growth plate where the cartilage template is first formed and then replaced by bone. The proliferation, hypertrophy, differentiation, and secretion into the extracellular matrix of chondrocytes in the growth plate lead to the formation of new cartilage, chondrogenesis (17). As new cartilage is continuously formed, the terminally differentiated chondrocytes undergo apoptosis; the metaphysis invades the growth plate with blood vessels and

[4] The abbreviations used are: SIRT1, sirtuin-1; ER, endoplasmic reticulum; PBA, phenylbutyric acid; UPR, unfolded protein response; OA, osteoarthritis; qPCR, quantitative PCR; BrdU, bromodeoxyuridine; THG, thapsigargin; TUNEL, terminal deoxynucleotidyltransferase-mediated dUTP nick end labeling; GAPDH, glyceraldehyde-3-phosphate dehydrogenase; ITS, insulin, transferrin, and sodium selenite.

bone cell precursors that remodel the cartilage into bone tissue (18).

Because of chondrocytes secreting large amounts of extracellular matrix during the process of endochondral ossification, the endoplasmic reticulum (ER) plays an important role in chondrocytes. In fact, a growing number of studies have recently revealed that maintaining ER homeostasis is crucial for skeletal development (19–21). We have recently demonstrated that autophagy deficiency triggers ER stress and inhibit growth-plate chondrogenesis via PERK–eIF-2α–CHOP pathway (22). More recently, Prola *et al.* (23) have shown that SIRT1 protects cardiomyocytes against ER stress–induced apoptosis via regulating the PERK–eIF-2α pathway. However, whether and how SIRT1 modulates ER stress response in the growth-plate chondrocytes has not been elucidated yet. Based on all these findings, we hypothesized that 1) SIRT1 facilitates longitudinal bone growth and growth-plate chondrogenesis and 2) such effects of SIRT1 are mediated by an unidentified pathway such as PERK–eIF-2α–CHOP.

We show that EX527 (a known specific SIRT1 inhibitor) inhibits metatarsal longitudinal growth and growth-plate chondrogenesis, with such effects being partly neutralized by phenylbutyric acid (PBA, a chemical chaperone known to attenuate ER stress). In addition, we evaluate the effects of EX527 or SIRT1 siRNA on cultured chondrocyte proliferation, hypertrophy, and apoptosis. Meanwhile, we observe that the inhibition of SIRT1 activity (by EX527 or SIRT1 siRNA) leads to the PERK–eIF-2α–CHOP axis of the ER stress response. Furthermore, we show SIRT1 regulates the PERK–eIF-2α–CHOP pathway partly through PERK deacetylation. Our results support the hypothesis that SIRT1 promotes growth-plate chondrogenesis via maintaining ER homeostasis in PERK–eIF-2α–CHOP–dependent manner.

Results

Effects of EX527 and PBA on metatarsal longitudinal growth

To determine whether SIRT1 regulates growth-plate chondrogenesis, we cultured fetal rat metatarsals for 3 days in serum-free medium in the presence of EX527 (0–100 μM), a specific SIRT1 inhibitor. During the 3 days of the culture period, 30 μM (the lowest growth inhibiting concentration) EX527 significantly inhibited metatarsal longitudinal growth (Fig. 1, *a* and *b*). To further confirm the findings of SIRT1 on longitudinal growth, we obtained metatarsal bones from conditional knockout mice (SIRT1 cartilage-specific cKO mice, generated using the Cre-loxP system). As expected, ablation of SIRT1 specific in chondrocytes inhibited metatarsal bones growth significantly after the 3 days of the culture (Fig. S1*A*). Immunohistochemical analysis of sections of 3 days metatarsal bones using the specific antibody against SIRT1 showed that the whole growth plate, including epiphyseal, proliferative, and hypertrophic chondrocyte, stains intensely for SIRT1, whereas 30 μM EX527 caused a significant decrease of SIRT1 expression in growth plate (Fig. S1*B*). Western blotting of lysates from cultured chondrocytes treated with EX527 confirmed that graded concentrations of EX527 caused a dose-dependent inhibition of SIRT1 expression, with a lowest inhibitory concentration of 30 μM (Fig. S2*A*). We also analyzed the effect of 30 μM EX527 on the expression of other sirtuin, SIRT2, in the metatarsal growth plate as well as in cultured chondrocyte. We found that there were no significant changes in the expression of SIRT2 in metatarsals (Fig. S1*C*) or chondrocytes (Fig. S2*A*) treated with 30 μM EX527, indicating that 30 μM EX527 could act specifically on SIRT1 without hitting other sirtuin.

Because we have previously demonstrated that the PERK–eIF-2α–CHOP axis of ER stress exerts an important role in growth-plate chondrogenesis (22), we sought to determine whether EX527 inhibited metatarsal longitudinal growth via inducing the PERK–eIF-2α–CHOP axis of ER stress. As expected, TEM analysis showed that the ER cisternae were dilated in growth-plate chondrocytes of EX527-treated metatarsals compared with control metatarsals (Fig. 1*e*). To confirm that inhibition of SIRT1 induced ER stress in chondrocytes, we then analyzed the expression of ER stress indicators in metatarsal growth plate by Western blotting and RT-qPCR. Western blotting of lysates from control and EX527-treated metatarsals confirmed EX527 significantly increased the phosphorylation of PERK and eIF-2α and the expression of CHOP compared with control metatarsals (Fig. 1*c* and Fig. S1*D*), and RT-qPCR also shows a similar pattern of expression (Fig. 1*d*). To further confirm the effects of EX527 on PERK–eIF-2α–CHOP axis of ER stress, chondrocytes isolated from rat fetal metatarsal rudiments were cultured in the presence of EX527 (0–100 μM). As shown in Fig. S2*A*, EX527 induced this pathway in a dose-dependent manner, with higher concentrations (30 and 100 μM) causing a statistically significant induction. To determine whether the inhibitory effects of EX527 on metatarsal longitudinal growth are mediated by ER stress, metatarsals were cultured in the absence or presence of 30 μM EX527, with or without 2 mM PBA, a chemical chaperone known to attenuate ER stress. As expected, PBA effectively attenuated ER stress induced by EX527 in chondrocytes, as assessed by expression of p-PERK, p-eIf-2α, ATF4, and CHOP by Western blotting (Fig. 1*f* and Fig. S1*E*) and RT-qPCR (Fig. 1*g*), respectively, and the addition of PBA partially neutralized the inhibitory effect of EX527 on metatarsal longitudinal growth (Fig. 1, *h* and *i*).

Effects of EX527 and PBA on growth-plate chondrogenesis

Because the rate of longitudinal bone growth depends primarily on the rate of growth-plate chondrogenesis, we evaluated the effects of EX527 on chondrocyte proliferation and hypertrophy. Treatment with EX527 significantly reduced the height of the epiphyseal and proliferative zones of the growth plate, where cell proliferation takes place (Fig. 2, *a* and *c*). Consistent with these findings, we examined the *in situ* incorporation of BrdU into the metatarsal rudiments at the end of the culture period and observed that EX527 significantly inhibited the incorporation of BrdU into the growth-plate epiphyseal and proliferative zones (Fig. 2*d*), whereas the addition of PBA partially neutralized the inhibitory effects of chondrocyte proliferation induced by EX527 (Fig. 2, *a*, *c*, and *d*). To assess chondrocyte hypertrophy, we examined the bone rudiments histologically. After 3 days in culture, 30 μM EX527 decreased the height of the growth-plate hypertrophic zone, whereas co-treatment with PBA reversed growth inhibition in hypertrophic

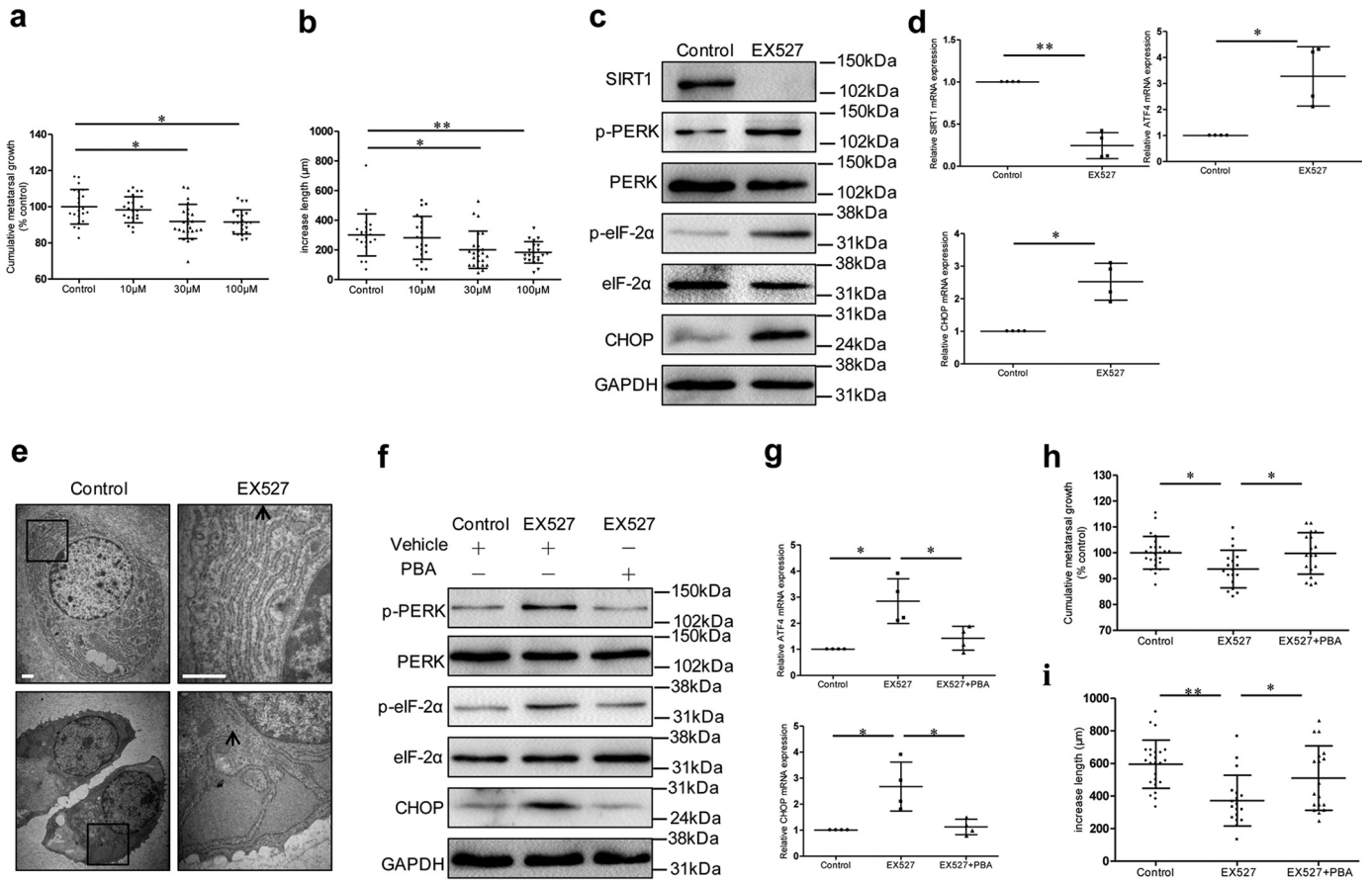

Figure 1. Effects of EX527 and PBA on metatarsal longitudinal growth. *a* and *b*, fetal rat metatarsals (20 days postconception) were cultured for 3 days in serum-free MEM containing graded concentrations of EX527 (0–100 μM, $n = 20$–24/group). Bone length was measured at the beginning and at the end of the experiments using an eyepiece micrometer in a dissecting microscope. At the end of 3 days in culture, protein and total RNA were obtained from metatarsals and processed as described under "Experimental procedures." *c*, the expression of SIRT1 and ER stress markers including PERK phosphorylation (*p-PERK*), eIF-2α phosphorylation (*p-eIF-2*α), and CHOP was detected by Western blotting. A representative blot from four independent experiments is presented for each protein. *d*, relative expression of SIRT1, ATF4, and CHOP was examined by real-time PCR, and the results are presented as gene expression levels in all groups normalized to controls. *e*, transmission EM of growth-plate chondrocytes displayed a normal structure of the rough ER in control metatarsals but unusually dilated ER cisternae in EX527-treated metatarsals. The *arrows* indicate ER. The *insets* show a high magnification of selected areas. *Scale bars*, 1 μm. *f*, fetal rat metatarsals (20 days postconception) were cultured for 3 days in serum-free MEM containing EX527 (30 μM, $n = 20$/group) and/or PBA (2 mM, $n = 20$/group). The expression of p-PERK, p-eIF-2α, and CHOP was detected by Western blotting. A representative blot from four independent experiments is presented for each protein. *g*, relative expression of ATF4 and CHOP was examined by real-time PCR. The results are presented as gene expression levels in all groups normalized to controls. *h* and *i*, bone length was measured at the beginning and at the end of the experiments using an eyepiece micrometer in a dissecting microscope. The data are expressed as the means ± S.D. in each scatter plots. *, $p < 0.05$; **, $p < 0.01$.

zone induced by EX527 (Fig. 2, *a* and *c*). Inhibition of chondrocyte hypertrophy by EX527 was also confirmed by Col10a1 immunohistochemistry (Fig. 2*b*). As shown in Fig. 2 (*b* and *e*), EX527 caused a marked decrease of Col10a1 expression, with such effect being partially abolished by the addition of PBA.

In light of the regulatory role of SIRT1 on apoptosis in other cell types, we evaluated the effects of EX527 on metatarsal growth-plate apoptosis by *in situ* cell death. EX527 caused a significant increase in cell death compared with control (Fig. 2*f*), with such effect being neutralized by PBA (Fig. 2*f*).

EX527 induced ER stress, inhibited proliferation and hypertrophy, and increased apoptosis in cultured primary chondrocytes

To further determine the interaction between SIRT1 and ER stress in chondrocyte, primary chondrocytes derived from rat fetal metatarsal rudiments were cultured in the absence or presence of 30 μM EX527. As expected, EX527 reduced both SIRT1 protein (assessed by Western blotting; Fig. 3*a* and Fig. S3*B*) and mRNA expression (assessed by RT-qPCR; Fig. 3*b*). Furthermore, chondrocytes treated with EX527 also exhibited ER stress, as evidenced by the induction of PERK and eIF-2α phosphorylation and up-regulation of the expression of CHOP (Fig. 3*a* and Fig. S3*B*), similar to what we found in metatarsal study (Fig. 1*c* and Fig. S1*C*). We then restored SIRT1 expression in EX527-treated chondrocytes by overexpression plasmid of SIRT1, and the transfection efficiency was validated by fluorescence microscope (Fig. S3*A*) and reconfirmed by Western blotting (Fig. 3*a*) and RT-qPCR (Fig. 3*b*). After transient transfection, we verified that restoration of SIRT1 expression could ameliorate ER stress induced by EX527 in chondrocytes as detected by Western blotting and RT-qPCR (Fig. 3, *a* and *b*).

Consistent with the observation in the metatarsal growth plate, EX527 significantly inhibited BrdU incorporation (Fig. 3*c*), as well as cyclin D1 and PCNA expression (Fig. 3*d* and Fig. S3*C*), with these effects being abolished by overexpression plasmid of SIRT1 (Fig. 3, *c* and *d*). With respect to apoptosis, overexpression of SIRT1 neutralized the pro-apoptotic effect of

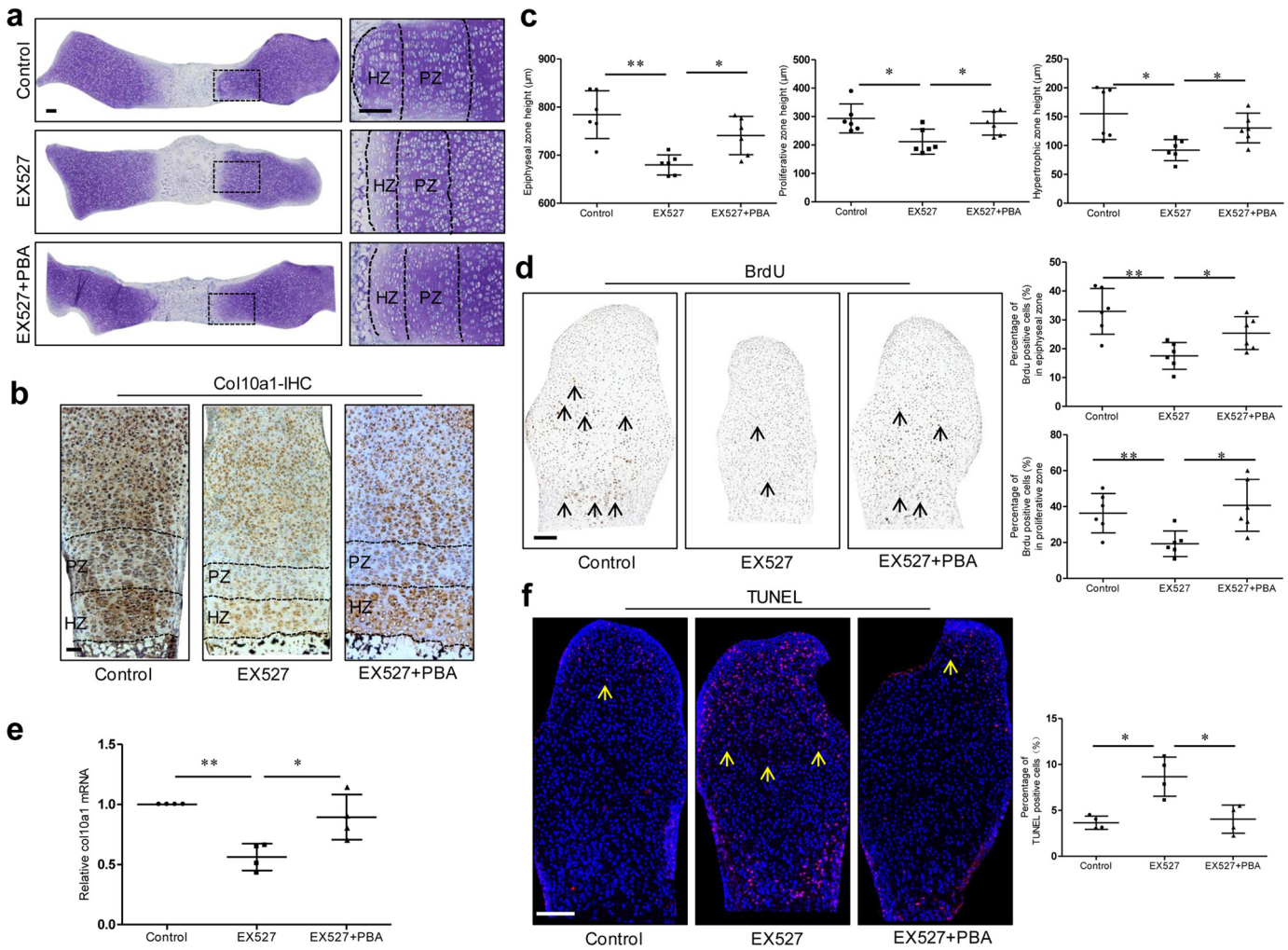

Figure 2. Effects of EX527 and PBA on chondrocyte proliferation, hypertrophy, and apoptosis in the metatarsal growth plate. At the end of the experimental period, metatarsal bones were fixed and paraffin-embedded, and 5- to 7-μm-thick longitudinal sections were obtained. *a*, representative images were obtained from each treatment of metatarsal bones stained with toluidine blue. *Insets* show a high magnification of selected areas. *Scale bars*, 100 μm. *PZ*, proliferative zone; *HZ*, hypertrophic zone. *b*, the expression of Col10a1 was detected in cultured metatarsals by immunohistochemistry. *Scale bars*, 50 μm. *c*, the heights of the epiphyseal, proliferative, and hypertrophic zones of the growth plate were quantitatively analyzed respectively ($n = 6$/group). After 3 days in culture, BrdU was added to the culture medium, and bone rudiments were incubated for an additional 2 h. *d*, representative images of the BrdU-positive cells. BrdU-positive cells were stained *brown* (indicated by the *arrow*). *Scale bars*, 100 μm. The number of BrdU-positive cells was analyzed separately for the epiphyseal zone and for the proliferative zone ($n = 6$/group). *e*, relative expression of Col10a1 was detected in growth-plate chondrocytes of metatarsal bones by real-time PCR. The results are presented as gene expression levels in all groups normalized to controls. *f*, representative images of the TUNEL-positive cells. TUNEL-positive cells were stained red fluorescence (indicated by the *arrow*). Quantification is shown on the *right*. The data are expressed as means ± S.D. in each scatter plot. *, $p < 0.05$; **, $p < 0.01$.

EX527, as analyzed by TUNEL assay (Fig. 3*e*) and Bcl-2/Bax ratio of protein expression (Fig. 3*f* and Fig. S3*D*). Lastly, to determine whether EX527 affects chondrocyte hypertrophy, we cultured chondrocytes with ITS for 7 days in the absence or presence of 30 μM EX527. Similarly, EX527 inhibited chondrocyte hypertrophy, as is evident by reduced Col10a1 and MMP13 expression (Fig. 3*g* and Fig. S3*E*), whereas the addition of 10 μM resveratrol, a SIRT1 activator, reversed the inhibition of Col10a1 and MMP13 expression induced by EX527 (Fig. 3*g* and Fig. S3*E*).

Effects of PBA on SIRT1 siRNA-induced inhibition of chondrocyte function

To further confirm whether inhibition of SIRT1 activity-mediated inhibition of chondrogenesis was caused by ER stress, chondrocytes were transfected with SIRT1 siRNA or control siRNA and cultured in the absence or presence of 2 mM PBA. Our finding indicated that PBA ameliorated ER stress induced by SIRT1 siRNA in chondrocytes as detected by Western blotting and RT-qPCR (Fig. 4, *a* and *b*, and Fig. S4*A*), thus partially neutralizing the inhibitory effects on chondrocyte proliferation (Fig. 4, *c* and *d*, and Fig. S4*B*) and hypertrophy (Fig. 4*g* and Fig. S4*D*) and diminishing the pro-apoptotic effect of SIRT1 siRNA (Fig. 4, *e* and *f*, and Fig. S4*C*).

Effects of CHOP siRNA on EX527-induced inhibition of chondrocyte function

Because we observed that SIRT1 inhibition or knockdown (treatment with EX527 or transfection with SIRT1 siRNA) mainly induced the PERK–eIF-2α–CHOP axis of the ER stress response in chondrocytes, we reasoned whether such inhibition of chondrocyte function was mediated by CHOP. To test this

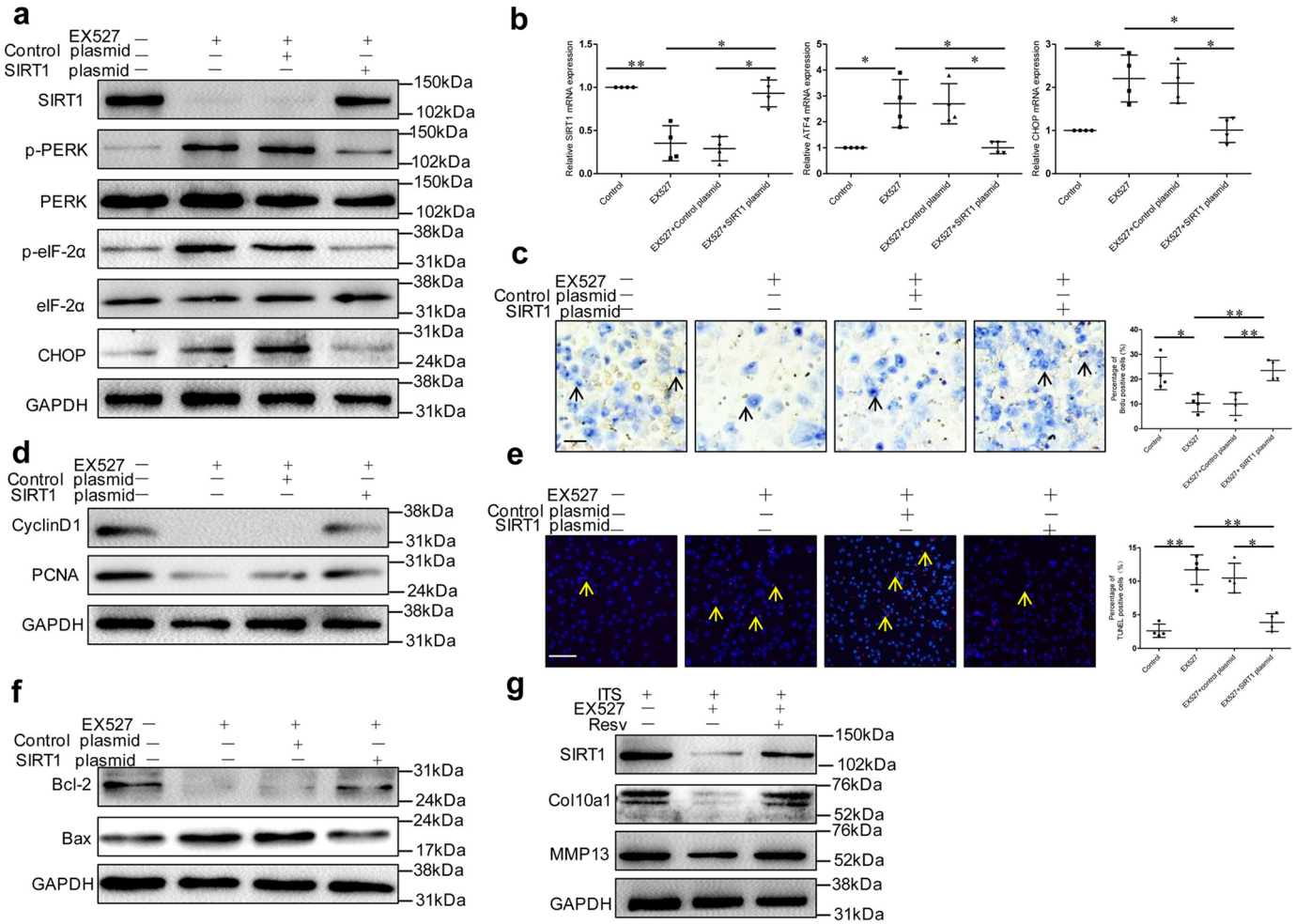

Figure 3. Effects of EX527 on proliferation, hypertrophy, and apoptosis in cultured primary chondrocytes. Chondrocytes were cultured for 48 h with or without EX527 (30 μM). For the rescue experiment, chondrocytes were pretreated with EX527 for 48 h and then transfected with either an empty vector (control plasmid) or a plasmid containing SIRT1 (SIRT1 plasmid) for additional 48 h. Both protein expression and mRNA expression were analyzed by Western blotting (*a*) and real-time PCR (*b*), respectively. *c*, primary chondrocytes were labeled with BrdU and prepared for staining as described under "Experimental procedures." Representative BrdU-positive cells are indicated by the *arrows*. *Scale bars*, 100 μm. Quantification is shown on the *right*. *d*, the expression of cyclin D1 and PCNA was detected by Western blotting in chondrocytes. A representative blot from four independent experiments is presented for each protein. *e*, primary chondrocytes were labeled with TUNEL. A representative TUNEL-positive cell is indicated by the *arrow*. *Scale bars*, 100 μm. Quantification is shown on the *right*. *f*, the expression of Bcl-2 and Bax was detected by Western blotting. A representative blot from three independent experiments is presented for each protein. *g*, chondrocytes were cultured with ITS for 7 days and incubated in the absence or presence of 30 μM EX527 and in combination with or without 10 μM resveratrol. At the end of the culture period, chondrocytes were harvested, lysed, electrophoresed, and immunoblotted for SIRT1, Col10a1 and MMP13, a representative blot from three independent experiments is presented for each protein. The data are expressed as means ± S.D. in each scatter plots. *, $p < 0.05$; **, $p < 0.01$.

possibility, CHOP siRNA was transfected in chondrocytes, and its validation was measured by the reduction of CHOP protein expression by Western blotting (Fig. 5*a* and Fig. S5*A*). The transfection of CHOP siRNA alone had minor effect on chondrocyte proliferation, hypertrophy, and apoptosis given that basal level of CHOP in normal chondrocyte is low. However, CHOP siRNA abolished the suppression of EX527 on chondrocyte proliferation assessed by BrdU incorporation (Fig. 5*b*), as well as cyclin D1 and PCNA protein expression (Fig. 5*c* and Fig. S5*B*), and hypertrophy assessed by Col10a1 and MMP13 protein expression (Fig. 5*g* and Fig. S5*D*), meanwhile, neutralized the pro-apoptotic effect of EX527, as analyzed by TUNEL assay (Fig. 5*d*) and Bcl-2/Bax ratio of protein expression (Fig. 5*e* and Fig. S5*C*).

In addition, it has been reported that CHOP may form heterodimers with C/EBP-β and act as a transdominant-negative inhibitor of C/EBP-β signaling (24), and C/EBP-β has also been indicated to regulate chondrocyte hypertrophy through interacting with RUNX2. Given this evidence, to explore the downstream mechanism that regulates chondrocyte hypertrophy, we performed RT-qPCR in EX527-treated chondrocytes with or without CHOP siRNA. Inhibition of SIRT1 decreased the mRNA levels of C/EBP-β and RUNX2, whereas treatment with CHOP siRNA partially abrogated such inhibitory effects (Fig. 5*f*), suggesting that CHOP may regulate chondrocyte hypertrophy through interaction with C/EBP-β and RUNX2.

SIRT1 interacts with and deacetylates PERK

It is known that SIRT1 could regulate protein activity through deacetylation on lysine residues. Therefore, to study the mechanism by which SIRT1 attenuates the PERK–eIF-2α–CHOP pathway to maintain ER homeostasis, proteins acety-

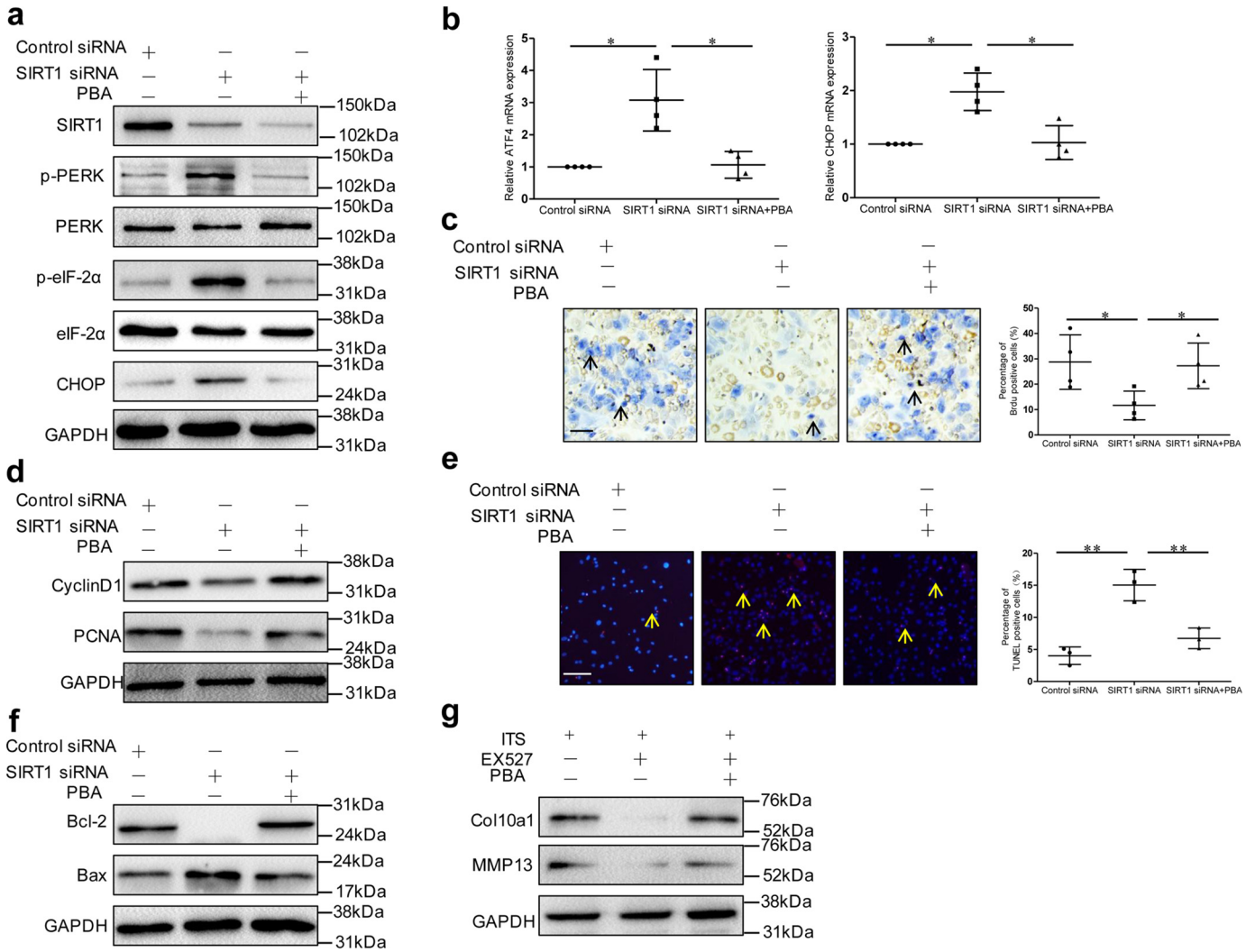

Figure 4. Effects of SIRT1 siRNA and PBA on proliferation, hypertrophy, and apoptosis in cultured primary chondrocytes. Chondrocytes transfected with control siRNA or SIRT1 siRNA cultured in the absence or presence of 2 mM PBA. *a*, at the end of the culture period, SIRT1, p-PERK, p-eIF-2α, and CHOP protein expression was determined by Western blotting. A representative blot from four independent experiments is presented for each protein. *b*, ATF4 and CHOP mRNA expression was examined by real-time PCR. The results are presented as gene expression levels in all groups normalized to controls. *c*, chondrocytes were labeled with BrdU and prepared for staining. Representative BrdU-positive cells are indicated by the *arrows*. *Scale bars*, 100 μm. Quantification is shown on the *right*. *d*, the expression of cyclin D1 and PCNA was detected by Western blotting. A representative blot from three independent experiments is presented for each protein. *e*, chondrocytes were labeled with TUNEL. Representative TUNEL-positive cells are indicated by the *arrows*. *Scale bars*, 100 μm. Quantification is shown on the *right*. *f*, Bcl-2 and Bax protein levels were determined by Western blotting. A representative blot from three independent experiments is presented for each protein. *g*, chondrocytes were treated with ITS for 7 days, cultured in the absence or presence of 30 μM EX527 and in combination with or without 2 mM PBA. At the end of the culture period, chondrocytes were harvested, lysed, electrophoresed, and immunoblotted for Col10a1 and MMP13. A representative blot from four independent experiments is presented for each protein. The data are expressed as means ± S.D. in each scatter plots. *, $p < 0.05$; **, $p < 0.01$.

lated on lysine residues were pulled down from primary chondrocyte lysates. In primary chondrocytes, only PERK was present in anti-acetyl lysine immunoprecipitates, whereas eIF-2α and CHOP were not detected, indicating that among the members of the PERK–eIF-2α–CHOP axis tested, PERK is the only lysine-acetylated protein (Fig. 6*a*). Moreover, reciprocal immunoprecipitation confirmed the acetylation of PERK on lysine residues (Fig. 6*b*). Of note, both depletion of SIRT1 with SIRT1 siRNA and inhibition of SIRT1 with EX527 significantly increased the acetylation level of PERK as shown in Fig. 6 (*c* and *d*). To determine whether SIRT1 directly interacts with PERK in chondrocytes, co-immunoprecipitation assays were carried out. Immunoprecipitation of endogenous SIRT1 from primary chondrocyte lysates co-precipitated PERK (Fig. 6*e*); meanwhile, the reverse experiments immunoprecipitating endogenous PERK and immunoblotting for SIRT1 (Fig. 6*e*) further confirmed their physical interaction. Interestingly, thapsigargin (THG), which induces ER stress by inhibiting sarco/endoplasmic reticulum calcium ATPases, increased the level of PERK acetylation (Fig. 6, *f* and *g*), and such level was similar when SIRT1 was inhibited by EX527 or SIRT1 siRNA (Fig. 6, *f* and *g*), indicating that SIRT1 limits the acetylation level of PERK to maintain ER homeostasis *in vitro*. Furthermore, in parallel with acetylation, the level of phosphorylation of PERK was also increased in chondrocytes treated with THG or treated with EX527 or SIRT1 siRNA (Fig. 6, *f* and *g*), suggesting a dynamic interplay between these two post-translational modifications. Collectively, these results showed that PERK is acetylated on

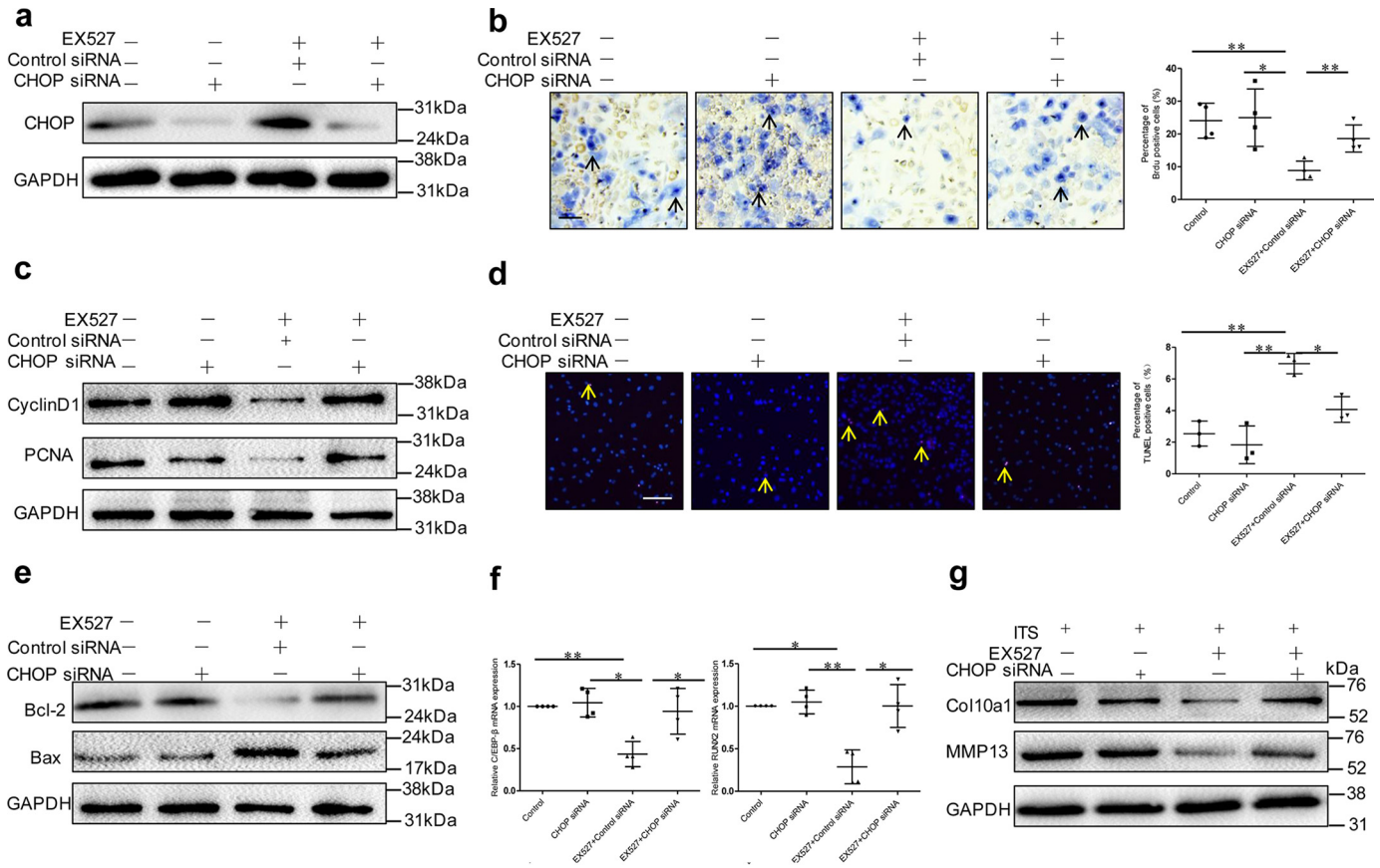

Figure 5. CHOP siRNA partially reverses EX527-mediated inhibition of chondrocyte proliferation and hypertrophy and neutralizes EX527-mediated pro-apoptotic effect. Chondrocytes were transfected with CHOP siRNA for 72 h or cultured with or without 30 μM EX527 and in combination with control or CHOP siRNA. *a*, the expression of CHOP was detected by Western blotting. A representative blot from four independent experiments is presented for each protein. *b*, chondrocytes were labeled with BrdU and prepared for staining. Representative BrdU-positive cells are indicated by the *arrow*. *Scale bars*, 100 μm. Quantification is shown on the *right*. *c*, cyclin D1 and PCNA protein expression was determined by Western blotting. A representative blot from four independent experiments is presented for each protein. *d*, chondrocytes were labeled with TUNEL. Representative TUNEL-positive cells are indicated by the *arrows*. *Scale bars*, 100 μm. Quantification is shown on the *right*. *e*, the expression of Bcl-2 and Bax was detected by Western blotting. A representative blot from three independent experiments is presented for each protein. *f*, relative expression of C/EBP-β and Runx2 was examined by real-time PCR. The results are presented as gene expression levels in all groups normalized to controls. *g*, chondrocytes were treated with ITS for 7 days, cultured in the absence or presence of EX527, and transfected with or without CHOP siRNA. At the end of the culture period, chondrocytes were harvested, lysed, electrophoresed, and immunoblotted for Col10a1 and MMP13. A representative blot from four independent experiments is presented for each protein. The data are expressed as means ± S.D. in each scatter plot. *, $p < 0.05$; **, $p < 0.01$.

one or more lysine residues and that this acetylation is regulated, at least in part, by SIRT1 to maintain ER homeostasis in chondrocytes.

Discussion

Recent evidence suggests that STRT1, which is considered a longevity factor, may be implicated in the regulation of longitudinal bone growth. SIRT1-null mice are significantly smaller than WT littermates during embryogenesis and postnatal stages, and they do not survive longer than 1 month postnatally (25). In addition, SIRT1-heterozygous knockout mice show reduced growth and shortened long bones (26), and they also exhibit metabolic impairments and reduced bone mass (27, 28). Furthermore, we have previously demonstrated a direct circadian regulation of Bmal1 in cartilage homeostasis mediated by SIRT1 (29). However, these findings provide only indirect evidence of SIRT1 regulating growth-plate function.

In the present study, we demonstrated that inhibition of SIRT1 caused a significant suppression of metatarsal longitudinal growth, which resulted from induction of the PERK–eIF-2α–CHOP axis of the ER stress response in growth-plate chondrocytes, causing inhibition of the two main cellular events of growth-plate chondrocyte proliferation and hypertrophy (30) and eventually leading to an inhibition of growth-plate chondrogenesis. Meanwhile, the ubiquitous localization of SIRT1 in metatarsal growth plate further supports the finding of a uniformly suppressed chondrogenesis throughout the growth plate. All these findings indicate that SIRT1 expressed in growth-plate chondrocytes facilitates chondrocyte proliferation and hypertrophy and prevents apoptosis.

Chondrocytes are known to have an increased ER burden caused by the synthesis and secretion of the large amount of extracellular matrix protein during development (19, 31, 32); they rely on the unfolded protein response (UPR) to maintain ER homeostasis. Previous studies in other cell types have shown that SIRT1 reduced the ER stress and apoptosis of brown adipocyte by inhibiting Smad3/ATF4 signal (33), and SIRT1 protects cardiomyocytes against ER stress-induced apoptosis by attenuating the PERK–eIF-2α pathway (23). Of note, we observed that ER cisternae were enlarged and distended in

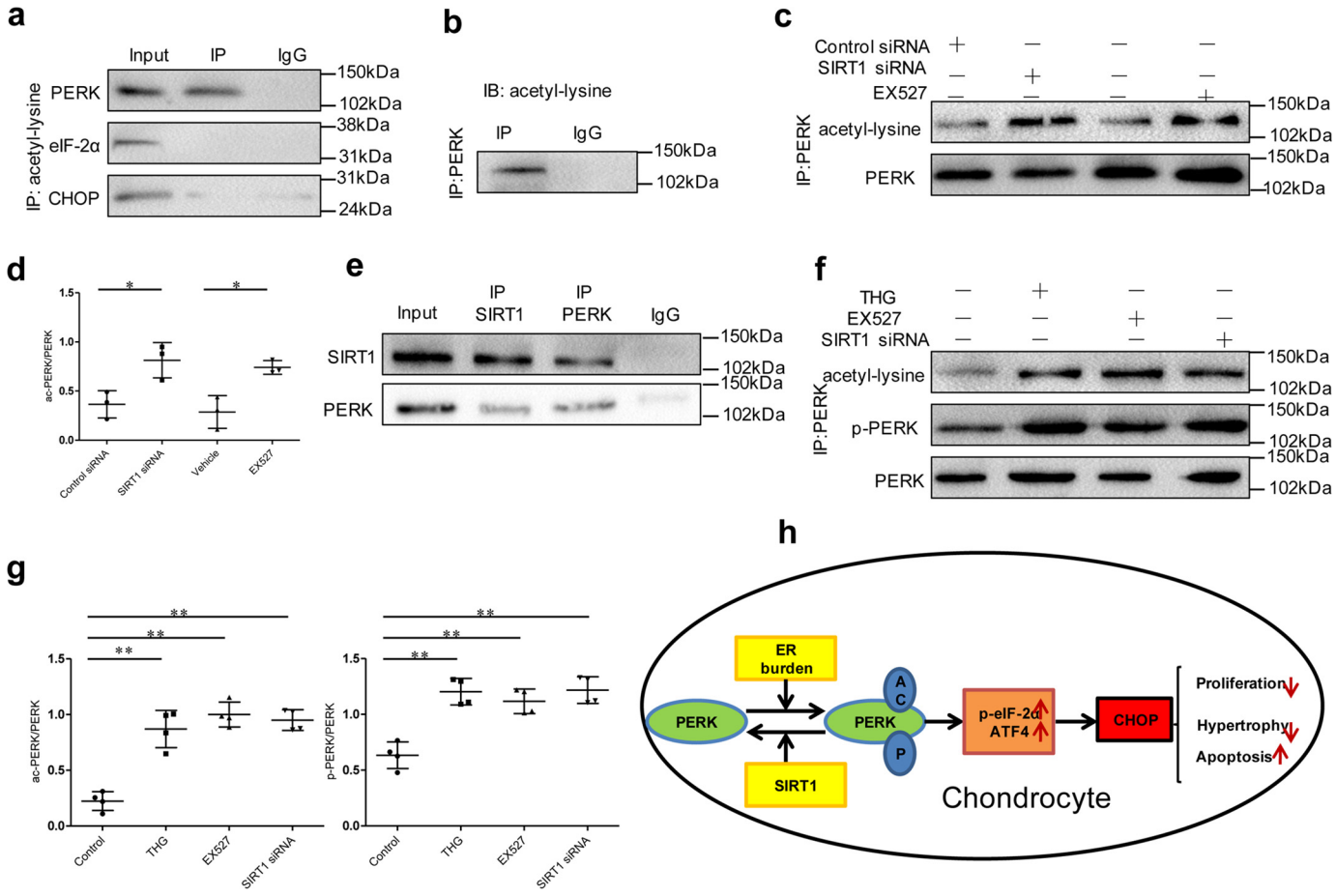

Figure 6. SIRT1 physically interacts with and deacetylates PERK. *a*, immunoprecipitation of acetylated proteins from chondrocyte lysate followed by immunoblotting with the indicated antibodies. *Input*, supernatant before immunoprecipitation; *IP*, immunoprecipitate; *IgG*, negative control. *b*, PERK was immunoprecipitated from chondrocyte lysate, and its level of acetylation was analyzed by immunoblotting with anti-acetyl-lysine antibody. *c* and *d*, PERK was immunoprecipitated from control or chondrocytes treated with EX527 (30 μM) or SIRT1 siRNA, and its level of acetylation was determined by immunoblotting with anti-acetyl-lysine antibody. The relative quantity of acetylated PERK was analyzed using ImageJ software and is shown in *d*. *e*, the physical interaction between endogenous SIRT1 and PERK was demonstrated by co-immunoprecipitation. SIRT1 was precipitated from chondrocyte lysate with anti-SIRT1 antibody and blotted with anti-PERK antibody, and vice versa. *f* and *g*, PERK was immunoprecipitated from control or chondrocytes treated with THG (80 nM) or EX527 (30 μM) or SIRT1 siRNA, and its levels of acetylation and phosphorylation were analyzed. The relative quantity of acetylated and phosphorylated PERK were analyzed using ImageJ software and is shown in *g*. A representative blot from three or four independent experiments is presented for each protein. The data are expressed as means ± S.D. in each scatter plots. *, $p < 0.05$; **, $p < 0.01$. *h*, proposed model of SIRT1 protection function in chondrocytes. SIRT1 protects chondrocytes against ER burden-induced injury and maintains ER homeostasis during the process of chondrogenesis.

growth-plate chondrocytes of EX527-treated metatarsals, indicating that SIRT1 may facilitate maintaining ER homeostasis in growth-plate chondrocytes. However, in embryonic fibroblasts, SIRT1 was reported to exert deleterious effects and to sensitize these cells to ER stress-induced apoptosis via regulating the IRE1 branch of the UPR through deacetylation of XBP1s (34). The discrepancies may reflect cell-type specificities including differentiation state.

Because we have recently demonstrated that the PERK–eIF-2α–CHOP axis of ER stress exerts an important role in chondrogenesis (22), we hypothesized that SIRT1 facilitates maintaining ER homeostasis and protects chondrocytes against severe ER stress by attenuating PERK–eIF-2α–CHOP pathway. Indeed, we show that inhibition of SIRT1 in metatarsals and chondrocytes results in hyperactivation of PERK–eIF-2α pathway. Furthermore, we observe that reduction of ER stress with PBA partially restored EX527 or STRT1 siRNA-induced inhibitory effect on metatarsal longitudinal growth and chondrocyte function (*i.e.* of proliferation, hypertrophy, and apoptosis). In addition, EX527-mediated impaired chondrocyte function was partly reversed in CHOP$^{-/-}$ cells, further supporting that SIRT1 mediates its protective effects, at least in part, by attenuation excessive ER stress via the PERK–eIF-2α–CHOP–dependent pathway.

The ability of cells to respond to ER stress is critical for cell survival, but chronic or irrecoverable levels of ER stress can lead to apoptosis (35). CHOP, a C/EBP homologous protein, also known as a pro-apoptotic factor, is understood to be a later event in the PERK–eIF-2α axis of UPR activation (36). CHOP can directly regulate death effectors, such as Bcl-2 and Bim, which subsequently render the cells more susceptible to apoptosis (37, 38). It was reported that CHOP deficiency promotes cell survival in an ER stress–related model of type 2 diabetes (39). In a murine OA model, chondrocyte death and cartilage degeneration are decreased in CHOP$^{-/-}$ mice (40), indicating that CHOP plays an important role in ER stress-induced apoptosis. Consistent with these findings, down-regulation of CHOP in chondrocytes could partly restore EX527-mediated

inhibition of chondrocyte proliferation and partly neutralize EX527-mediated pro-apoptotic effect. In addition to regulating apoptosis, CHOP can form heterodimers with C/EBP-β and act as a transdominant-negative inhibitor of C/EBP-β signaling (24). Several lines of evidence have implicated C/EBP-β as a key regulator in the transition of chondrocytes from proliferation to hypertrophy (41, 42), and C/EBP-β interacts cooperatively with GADD45-β and RUNX2 to promote chondrocyte hypertrophy and growth-plate matrix remodeling and turnover via up-regulation of the expression of key markers of chondrocyte maturation including Col10a1 and MMP13 (43, 44). Overall, our results support the hypothesis that SIRT1 inhibition, coupled with PERK–eIF-2α–CHOP axis of the ER stress and down-regulation of C/EBP-β and RUNX2 transcriptional activity, might result in impaired expression of Col10a1 and MMP13 for chondrocyte hypertrophy.

Although autophosphorylation of PERK has been intensively studied, the understanding of the molecular events regulating its autophosphorylation is poorly documented. Interaction of SIRT1 with eIF-2α has been shown in HeLa cells and cardiomyocytes (23, 45); however, no evidence was reported on PERK acetylation/deacetylation. In our study, we found that as a lysine-acetylated protein, PERK physically interacts with SIRT1 and being deacetylated on its lysine residues. In chondrocytes, inhibition of SIRT1 promotes both hyperacetylation and phosphorylation of PERK and then triggers the PERK–ATF4–CHOP axis of the ER stress, suggesting that SIRT1 may regulate PERK–eIF-2α UPR pathway via deacetylation of PERK.

It is known that the activity of numerous targets of SIRT1 is regulated both by deacetylation and by phosphorylation, including PGC-1α, p53, FOXO, and Beclin1 (6, 46); however, the interplay between these two post-translational modifications is not fully understood. Our observations that PERK acetylation occurred earlier than phosphorylation when SIRT1 is inhibited (Fig. S6) further support the notion that SIRT1, by regulating the level of acetylation of PERK, may regulate its level of phosphorylation and thus its activity. Although additional studies are needed to clarify the relationship between acetylation and phosphorylation of PERK, our data provide a clue as to how SIRT1 attenuates PERK–eIF-2α pathway in chondrocytes.

In conclusion, we have demonstrated that SIRT1 facilitates longitudinal bone growth and growth-plate chondrogenesis through regulation the PERK–eIF-2a–CHOP axis of the ER stress (*schematic diagram* in Fig. 6*h*). This study is the first to analyze the function of SIRT1 in growth plate and extends our understanding of how SIRT1 interacts with key UPR pathways controlling growth-plate chondrogenesis.

Experimental procedures

Whole metatarsal culture

The second, third, and fourth metatarsal bones were isolated from Sprague–Dawley rat embryos (20 days postcoitum) and cultured individually in 24-well plates. Each well contained 0.5 ml of minimum essential medium (HyClone) with 0.2% BSA (Sigma), 100 units/ml penicillin, 100 μg/ml streptomycin (HyClone), and 50 μg/ml ascorbic acid (Sigma). Bone rudiments were cultured for 3 days in a humidified incubator with 5% CO_2 in air at 37 °C. The medium was changed on day 2. During the 3-day culture period, metatarsals were cultured in the absence or presence of EX527 (30 μM, Sigma, catalog no. E7034), with or without PBA (2 mM, Sigma, catalog no. SML0309).

Measurement of longitudinal growth

The length of each bone rudiment was measured under a dissecting microscope, using an eyepiece micrometer. To calculate the metatarsal growth rate, length measurements were performed at the beginning and at the end of the experiments. For each treatment group, 24 metatarsal bones isolated from 4 rat fetuses of the same litter were used. To confirm the effect of SIRT1 on metatarsal longitudinal growth, we performed three independent experiments from three pregnant mothers.

Quantitative histological analysis

At the end of the culture period, metatarsals were fixed in 4% phosphate-buffered paraformaldehyde overnight. After routine processing, three 5–7-μm-thick longitudinal sections were obtained from each metatarsal bone and stained with toluidine blue. From each of the three sections, we measured the height of the epiphyseal zone, the proliferative zone, and the hypertrophic zone and calculated the average value. In the metatarsal growth plate, the epiphyseal zone is characterized by small and rounded cells, irregularly arranged in the cartilage matrix. The proliferative zone comprises cells with a flattened shape, arranged in columns parallel to the longitudinal axis of the bone. Eventually, chondrocytes, which are located farthest from the epiphyseal zone, stop replicating and enlarge to become hypertrophic chondrocytes (defined by a height of $\geq$9 μm). All measurements were performed by a single observer blinded to the treatment regimen.

Immunohistochemistry

To detect SIRT1 and type X collagen (Col10a1) expression in the metatarsal bones, metatarsals were fixed in 4% phosphate-buffered paraformaldehyde overnight. After routine processing, 5–7-μm-thick longitudinal sections were obtained. The sections were immunostained with SPlink detection kits (Zhongshan Biotechnologies, Beijing, China; catalog no. SP-9001). Briefly, the sections were treated with 0.25% trypsin for 10 min at 37 °C for antigen retrieval after the pretreatment of 3% H_2O_2 and then were blocked using 5% goat serum for 15 min at room temperature. Afterward, the sections were incubated with designated primary antibodies overnight at 4 °C. Antibodies included mouse anti-SIRT1 antibody at a dilution of 1:200 (Abcam, ab110304) and rabbit anti-Col10a1 antibody at a dilution of 1:200 (Abcam, ab58632). After three rinses with PBS, the sections were incubated with respective secondary antibodies for 15 min at room temperature. Finally, the sections were counterstained with hematoxylin.

BrdU incorporation

Cultured metatarsal bones were exposed to BrdU (1:100, Invitrogen, catalog no. 00-0103) for an additional 2 h before the

end of culture period. The BrdU-labeled cells were visualized utilizing a BrdU labeling kit (Invitrogen, catalog no. 93-3943) according to the manufacturer's instructions. Primary chondrocytes were exposed to BrdU (1:1000, Roche) for 15 min before fixation. The BrdU-labeled cells were visualized utilizing a BrdU labeling and detection kit (Roche, catalog no. 11299964001) according to the manufacturer's instructions. The percentage of BrdU-positive cells was calculated as the number of BrdU-labeled cells per grid divided by the total number of cells per grid. For each sample, the fraction of labeled cells in three distinct grid locations was calculated and averaged. All determinations were made by the same observer blinded to the treatment category.

TUNEL assay

Apoptotic cells in the metatarsal growth plate and primary chondrocytes were identified by an *in situ* cell death detection kit (Roche, catalog no. 12156792910), according to the manufacturer's instructions. The nuclei were counterstained with DAPI. TUNEL-positive cells were stained red fluorescence. The percentage of TUNEL-positive cells was calculated as the number of TUNEL-labeled cells per grid divided by the total number of cells per grid. For each sample, the fraction of labeled cells in three distinct grid locations was calculated and averaged. All determinations were made by the same observer blinded to the treatment category.

EM analysis

Metatarsal bones were fixed in 2% glutaraldehyde and embedded in epoxy resin (Epon). Ultrathin sections (80 nm) were stained with aqueous uranyl acetate and lead citrate and examined with a JEOL 2000EX transmission EM (JEOL).

Primary chondrocyte culture

The cartilaginous portions of metatarsal bones isolated from Sprague–Dawley rat embryos (20 days postcoitum) were dissected, rinsed in PBS, and then incubated in 0.2% collagenase (Sigma, catalog no. C6885) for 2 h. The cell suspension was aspirated repeatedly and filtered through a 70-μm cell strainer, rinsed first in PBS and then in serum-free DMEM, and counted. Chondrocytes were seeded at a density of 2×10^6 cell/ml in DMEM with 100 units/ml penicillin, 100 μg/ml streptomycin, 50 μg/ml ascorbic acid, and 10% FBS (Gibco). The culture medium was changed at 72-h intervals. ITS-inducing culture was initiated at chondrocytes reaching 70–80% confluence by adding ITS (Sigma, catalog no. I3146) (1:100) into the culture medium.

siRNA transfection

Chondrocytes were transfected with pools of siRNAs targeted for SIRT1 (Santa Cruz, catalog no. sc-108043) or CHOP (Santa Cruz, catalog no. sc-156118), and a pool of siRNAs consisting of scrambled sequences was similarly transfected as control siRNA (Santa Cruz). siRNA was introduced to cells using Lipofectamine 2000 (Invitrogen, catalog no. 11668027), according to the procedure recommended by the manufacturer. The transfected cells were cultured in DMEM containing 10% FBS for 48 h after transfection.

SIRT1 plasmid transfection

Chondrocytes were transfected with the expression plasmid for SIRT1 or a control plasmid (Genechem Co., Shanghai, China) for 48 h. The expression vector was introduced to cells using Lipofectamine LTX (Invitrogen, catalog no. 15338100) according to the procedure recommended by the manufacturer.

Western blotting

Whole-cell extracts were prepared by lysing cells with the radioimmune precipitation assay buffer. Proteins were separated by 8–15% SDS-PAGE gel, and the separated proteins were transferred onto a polyvinylidene difluoride membranes (Millipore) and were probed with the following primary antibodies: rabbit monoclonal antibodies against SIRT1 (Cell Signaling, catalog no. 9475), PERK (Cell Signaling, catalog no. 3192), Phospho-eIF-2α (Cell Signaling, catalog no. 3398), CHOP (Cell Signaling, catalog no. 5554), rabbit polyclonal antibodies against phospho-PERK (Santa Cruz, catalog no. sc-32577), Bcl-2 (Santa Cruz, catalog no. sc-492), Bax (Santa Cruz, catalog no. sc-6236), Col10a1 (Abcam, catalog no. ab58632), MMP13 (Abcam, catalog no. ab39012), mouse monoclonal antibodies against eIF-2α (Santa Cruz, catalog no. sc-133132), cyclin D1 (Santa Cruz, catalog no. sc-450), PCNA (Santa Cruz, catalog no. sc-25280), and GAPDH (Santa Cruz, catalog no. sc-365062). At last, the blots were visualized by an ECL detection system (Millipore) with a horseradish peroxidase-conjugated secondary antibody. A representative blot from three independent experiments is presented for each protein.

Immunoprecipitation

Cytoplasmic lysate (200 μg) was incubated for 2 h at 4 °C with the corresponding antibodies coupled to 20 μl of packed protein A+G-Sepharose beads (Santa Cruz, catalog no. sc-2002). Immune complexes were resolved by means of SDS-PAGE and immunoblotted with the indicated antibodies. To analyze the level of PERK acetylation, chondrocyte lysates were immunoprecipitated using anti-PERK antibody (Cell Signaling, catalog no. 3192), and then immunoprecipitated proteins were run on SDS-PAGE and immunoblotted with anti-PERK and anti-acetyl lysine antibody (Santa Cruz, catalog no. sc-32268), respectively.

RNA extraction and real-time PCR

Total RNA from cultured chondrocytes was isolated by TRIzol reagent (Invitrogen, catalog no. 15596-026) according to the manufacturer's instruction. The recovered RNA was further processed using RevertAid first strand cDNA synthesis kit (Thermo, catalog no. K1621) to produce cDNA in accordance with the manufacturer's instructions. The cDNA products were directly used for PCR or stored at −80 °C for later analysis. Real-time quantitative PCR was performed in the MJ mini real-time PCR detection system using SYBR Premix Ex Taq™ II (Takara, catalog no. RR047A). Primers were as follows: rat GAPDH (forward, 5′-TGA CGC TGG GGC TGG CAT TG-3′; reverse, 5′-GCT CTT GCT GGG GCT GGT GG-3′); rat SIRT1 (forward, 5′-TCG TGG AGA CAT TTT TAA TCA GG-3′;

reverse, 5′-GCT TCA TGA TGG CAA GTG G-3′), rat ATF4 (forward, 5′-TCT GCT TAT ATT ACT CTA ACC-3′; reverse, 5′-GAG AAC CAC GAG GAA CAC C-3′), rat CHOP (forward, 5′-CTC TGA CTG GAA TCT GGA GAG TG-3′; reverse, 5′-CTG AGT CAT TGC CTT TCT CCT TCG-3′), rat C/EBP-β (forward, 5′-GAC AAG CAC AGC GAC GAG TA-3′; reverse, 5′-GTG CTG CGT CTC CAG GTT-3′), rat RUNX2 (forward, 5′-CCT TCC CTC CGA GAC CCT AA-3′; reverse, 5′-ATG GCT GCT CCC TTC TGA AC-3′). Each experiment was performed in duplicate, and experiments were repeated four times independently. A dissociation curve analysis was conducted for each qPCR. Expression levels of the target gene were evaluated using a relative quantification approach ($2^{-\Delta\Delta Ct}$ method) against GAPDH levels.

Study approval

Animal care was approved by the Animal Experiment Administration Committee of the Medicine of Xi'an Jiaotong University in Shannxi, China.

Statistics

Statistical analysis was performed with the SPSS 17.0 software (SPSS Inc., Chicago, IL). All the experiments were repeated three or four times independently, and the data are presented as mean ± S.D. Statistical analysis was performed using two-tailed Student's *t* tests for two groups and one-way analysis of variance for more than two groups. *p* values less than 0.05 were considered statistically significant.

Author contributions—S. W., H. S., X. K., and W. Y. designed the study; S. W., X. K., X. J., and R. W. collected the data; S. W., X. K., D. F., and H. L. analyzed the data; S. W., X. K., W. Y., and T. X. interpreted the data; S. W., H. S., X. K., and W. Y. drafted the manuscript; all authors approved the final version of the manuscript; and S. W. and H. S. take responsibility for the integrity of the data and the accuracy of the data analysis.

References

1. Vaquero, A., Sternglanz, R., and Reinberg, D. (2007) NAD^+-dependent deacetylation of H4 lysine 16 by class III HDACs. *Oncogene* **26,** 5505–5520 CrossRef Medline
2. Vaziri, H., Dessain, S. K., Ng Eaton, E., Imai, S. I., Frye, R. A., Pandita, T. K., Guarente, L., and Weinberg, R. A. (2001) hSIR2(SIRT1) functions as an NAD-dependent p53 deacetylase. *Cell* **107,** 149–159 CrossRef Medline
3. Motta, M. C., Divecha, N., Lemieux, M., Kamel, C., Chen, D., Gu, W., Bultsma, Y., McBurney, M., and Guarente, L. (2004) Mammalian SIRT1 represses forkhead transcription factors. *Cell* **116,** 551–563 CrossRef Medline
4. Yeung, F., Hoberg, J. E., Ramsey, C. S., Keller, M. D., Jones, D. R., Frye, R. A., and Mayo, M. W. (2004) Modulation of NF-κB-dependent transcription and cell survival by the SIRT1 deacetylase. *EMBO J.* **23,** 2369–2380 CrossRef Medline
5. Liang, F., Kume, S., and Koya, D. (2009) SIRT1 and insulin resistance. *Nat. Rev. Endocrinol.* **5,** 367–373 CrossRef Medline
6. Haigis, M. C., and Sinclair, D. A. (2010) Mammalian sirtuins: biological insights and disease relevance. *Annu. Rev. Pathol.* **5,** 253–295 CrossRef Medline
7. Blander, G., and Guarente, L. (2004) The Sir2 family of protein deacetylases. *Annu. Rev. Biochem.* **73,** 417–435 CrossRef Medline
8. Sauve, A. A., Wolberger, C., Schramm, V. L., and Boeke, J. D. (2006) The biochemistry of sirtuins. *Annu. Rev. Biochem.* **75,** 435–465 CrossRef Medline
9. Dvir-Ginzberg, M., Gagarina, V., Lee, E. J., and Hall, D. J. (2008) Regulation of cartilage-specific gene expression in human chondrocytes by SirT1 and nicotinamide phosphoribosyltransferase. *J. Biol. Chem.* **283,** 36300–36310 CrossRef Medline
10. Hong, E. H., Lee, S. J., Kim, J. S., Lee, K. H., Um, H. D., Kim, J. H., Kim, S. J., Kim, J. I., and Hwang, S. G. (2010) Ionizing radiation induces cellular senescence of articular chondrocytes via negative regulation of SIRT1 by p38 kinase. *J. Biol. Chem.* **285,** 1283–1295 CrossRef Medline
11. Takayama, K., Ishida, K., Matsushita, T., Fujita, N., Hayashi, S., Sasaki, K., Tei, K., Kubo, S., Matsumoto, T., Fujioka, H., Kurosaka, M., and Kuroda, R. (2009) SIRT1 regulation of apoptosis of human chondrocytes. *Arthritis Rheum.* **60,** 2731–2740 CrossRef Medline
12. Gagarina, V., Gabay, O., Dvir-Ginzberg, M., Lee, E. J., Brady, J. K., Quon, M. J., and Hall, D. J. (2010) SirT1 enhances survival of human osteoarthritic chondrocytes by repressing protein tyrosine phosphatase 1B and activating the insulin-like growth factor receptor pathway. *Arthritis Rheum.* **62,** 1383–1392 CrossRef Medline
13. Fujita, N., Matsushita, T., Ishida, K., Kubo, S., Matsumoto, T., Takayama, K., Kurosaka, M., and Kuroda, R. (2011) Potential involvement of SIRT1 in the pathogenesis of osteoarthritis through the modulation of chondrocyte gene expressions. *J. Orthop. Res.* **29,** 511–515 CrossRef Medline
14. Matsuzaki, T., Matsushita, T., Takayama, K., Matsumoto, T., Nishida, K., Kuroda, R., and Kurosaka, M. (2014) Disruption of Sirt1 in chondrocytes causes accelerated progression of osteoarthritis under mechanical stress and during ageing in mice. *Ann. Rheum. Dis.* **73,** 1397–1404 CrossRef Medline
15. Lemieux, M. E., Yang, X., Jardine, K., He, X., Jacobsen, K. X., Staines, W. A., Harper, M. E., and McBurney, M. W. (2005) The Sirt1 deacetylase modulates the insulin-like growth factor signaling pathway in mammals. *Mech. Ageing Dev.* **126,** 1097–1105 CrossRef Medline
16. Gabay, O., Sanchez, C., Dvir-Ginzberg, M., Gagarina, V., Zaal, K. J., Song, Y., He, X. H., and McBurney, M. W. (2013) Sirtuin 1 enzymatic activity is required for cartilage homeostasis *in vivo* in a mouse model. *Arthritis Rheum.* **65,** 159–166 CrossRef Medline
17. Lee, N. K., Sowa, H., Hinoi, E., Ferron, M., Ahn, J. D., Confavreux, C., Dacquin, R., Mee, P. J., McKee, M. D., Jung, D. Y., Zhang, Z., Kim, J. K., Mauvais-Jarvis, F., Ducy, P., and Karsenty, G. (2007) Endocrine regulation of energy metabolism by the skeleton. *Cell* **130,** 456–469 CrossRef Medline
18. Wu, S., Yoshiko, Y., and De Luca, F. (2006) Stanniocalcin 1 acts as a paracrine regulator of growth plate chondrogenesis. *J. Biol. Chem.* **281,** 5120–5127 CrossRef Medline
19. Saito, A., Hino, S., Murakami, T., Kanemoto, S., Kondo, S., Saitoh, M., Nishimura, R., Yoneda, T., Furuichi, T., Ikegawa, S., Ikawa, M., Okabe, M., and Imaizumi, K. (2009) Regulation of endoplasmic reticulum stress response by a BBF2H7-mediated Sec23a pathway is essential for chondrogenesis. *Nat. Cell Biol.* **11,** 1197–1204 CrossRef Medline
20. Wang, W., Lian, N., Li, L., Moss, H. E., Wang, W., Perrien, D. S., Elefteriou, F., and Yang, X. (2009) Atf4 regulates chondrocyte proliferation and differentiation during endochondral ossification by activating Ihh transcription. *Development* **136,** 4143–4153 CrossRef Medline
21. Cameron, T. L., Gresshoff, I. L., Bell, K. M., Piróg, K. A., Sampurno, L., Hartley, C. L., Sanford, E. M., Wilson, R., Ermann, J., Boot-Handford, R. P., Glimcher, L. H., Briggs, M. D., and Bateman, J. F. (2015) Cartilage-specific ablation of XBP1 signaling in mouse results in a chondrodysplasia characterized by reduced chondrocyte proliferation and delayed cartilage maturation and mineralization. *Osteoarthritis Cartilage* **23,** 661–670 CrossRef Medline
22. Kang, X., Yang, W., Feng, D., Jin, X., Ma, Z., Qian, Z., Xie, T., Li, H., Liu, J., Wang, R., Li, F., Li, D., Sun, H., and Wu, S. (2017) Cartilage-specific autophagy deficiency promotes ER stress and impairs chondrogenesis in PERK–ATF4–CHOP-dependent manner. *J. Bone Miner. Res.* **32,** 2128–2141 CrossRef Medline
23. Prola, A., Pires Da Silva, J., Guilbert, A., Lecru, L., Piquereau, J., Ribeiro, M., Mateo, P., Gressette, M., Fortin, D., Boursier, C., Gallerne, C., Caillard, A., Samuel, J. L., François, H., Sinclair, D. A., *et al.* (2017) SIRT1 protects the heart from ER stress-induced cell death through eIF2α deacetylation. *Cell Death Differ.* **24,** 343–356 CrossRef Medline

24. Ron, D., and Habener, J. F. (1992) CHOP, a novel developmentally regulated nuclear protein that dimerizes with transcription factors C/EBP and LAP and functions as a dominant-negative inhibitor of gene transcription. *Genes Dev.* **6,** 439–453 CrossRef Medline
25. McBurney, M. W., Yang, X., Jardine, K., Hixon, M., Boekelheide, K., Webb, J. R., Lansdorp, P. M., and Lemieux, M. (2003) The mammalian SIR2α protein has a role in embryogenesis and gametogenesis. *Mol. Cell. Biol.* **23,** 38–54 CrossRef Medline
26. Gabay, O., Oppenhiemer, H., Meir, H., Zaal, K., Sanchez, C., and Dvir-Ginzberg, M. (2012) Increased apoptotic chondrocytes in articular cartilage from adult heterozygous SirT1 mice. *Ann. Rheum. Dis.* **71,** 613–616 CrossRef Medline
27. Xu, F., Gao, Z., Zhang, J., Rivera, C. A., Yin, J., Weng, J., and Ye, J. (2010) Lack of SIRT1 (mammalian Sirtuin 1) activity leads to liver steatosis in the SIRT1+/- mice: a role of lipid mobilization and inflammation. *Endocrinology* **151,** 2504–2514 CrossRef Medline
28. Cohen-Kfir, E., Artsi, H., Levin, A., Abramowitz, E., Bajayo, A., Gurt, I., Zhong, L., D'Urso, A., Toiber, D., Mostoslavsky, R., and Dresner-Pollak, R. (2011) Sirt1 is a regulator of bone mass and a repressor of Sost encoding for sclerostin, a bone formation inhibitor. *Endocrinology* **152,** 4514–4524 CrossRef Medline
29. Yang, W., Kang, X., Liu, J., Li, H., Ma, Z., Jin, X., Qian, Z., Xie, T., Qin, N., Feng, D., Pan, W., Chen, Q., Sun, H., and Wu, S. (2016) Clock gene Bmal1 modulates human cartilage gene expression by crosstalk with Sirt1. *Endocrinology* **157,** 3096–3107 CrossRef Medline
30. Aharinejad, S., Marks, S. C., Jr., Böck, P., MacKay, C. A., Larson, E. K., Tahamtani, A., Mason-Savas, A., and Firbas, W. (1995) Microvascular pattern in the metaphysis during bone growth. *Anat. Rec.* **242,** 111–122 CrossRef Medline
31. Murakami, T., Saito, A., Hino, S., Kondo, S., Kanemoto, S., Chihara, K., Sekiya, H., Tsumagari, K., Ochiai, K., Yoshinaga, K., Saitoh, M., Nishimura, R., Yoneda, T., Kou, I., Furuichi, T., *et al.* (2009) Signalling mediated by the endoplasmic reticulum stress transducer OASIS is involved in bone formation. *Nat. Cell Biol.* **11,** 1205–1211 CrossRef Medline
32. Saito, A., Ochiai, K., Kondo, S., Tsumagari, K., Murakami, T., Cavener, D. R., and Imaizumi, K. (2011) Endoplasmic reticulum stress response mediated by the PERK–eIF2α–ATF4 pathway is involved in osteoblast differentiation induced by BMP2. *J. Biol. Chem.* **286,** 4809–4818 CrossRef Medline
33. Liu, Z., Gu, H., Gan, L., Xu, Y., Feng, F., Saeed, M., and Sun, C. (2017) Reducing Smad3/ATF4 was essential for Sirt1 inhibiting ER stress-induced apoptosis in mice brown adipose tissue. *Oncotarget* **8,** 9267–9279 Medline
34. Wang, F. M., Chen, Y. J., and Ouyang, H. J. (2011) Regulation of unfolded protein response modulator XBP1s by acetylation and deacetylation. *Biochem. J.* **433,** 245–252 CrossRef Medline
35. Tabas, I., and Ron, D. (2011) Integrating the mechanisms of apoptosis induced by endoplasmic reticulum stress. *Nat. Cell Biol.* **13,** 184–190 CrossRef Medline
36. Woehlbier, U., and Hetz, C. (2011) Modulating stress responses by the UPRosome: a matter of life and death. *Trends Biochem. Sci.* **36,** 329–337 CrossRef Medline
37. Marciniak, S. J., Yun, C. Y., Oyadomari, S., Novoa, I., Zhang, Y., Jungreis, R., Nagata, K., Harding, H. P., and Ron, D. (2004) CHOP induces death by promoting protein synthesis and oxidation in the stressed endoplasmic reticulum. *Genes Dev.* **18,** 3066–3077 CrossRef Medline
38. McCullough, K. D., Martindale, J. L., Klotz, L. O., Aw, T. Y., and Holbrook, N. J. (2001) Gadd153 sensitizes cells to endoplasmic reticulum stress by down-regulating Bcl2 and perturbing the cellular redox state. *Mol. Cell. Biol.* **21,** 1249–1259 CrossRef Medline
39. Song, B., Scheuner, D., Ron, D., Pennathur, S., and Kaufman, R. J. (2008) Chop deletion reduces oxidative stress, improves β cell function, and promotes cell survival in multiple mouse models of diabetes. *J. Clin. Invest.* **118,** 3378–3389 CrossRef Medline
40. Uehara, Y., Hirose, J., Yamabe, S., Okamoto, N., Okada, T., Oyadomari, S., and Mizuta, H. (2014) Endoplasmic reticulum stress-induced apoptosis contributes to articular cartilage degeneration via C/EBP homologous protein. *Osteoarthritis Cartilage* **22,** 1007–1017 CrossRef Medline
41. Ushijima, T., Okazaki, K., Tsushima, H., and Iwamoto, Y. (2014) CCAAT/enhancer-binding protein beta regulates the repression of type II collagen expression during the differentiation from proliferative to hypertrophic chondrocytes. *J. Biol. Chem.* **289,** 2852–2863 CrossRef Medline
42. Hirata, M., Kugimiya, F., Fukai, A., Ohba, S., Kawamura, N., Ogasawara, T., Kawasaki, Y., Saito, T., Yano, F., Ikeda, T., Nakamura, K., Chung, U. I., and Kawaguchi, H. (2009) C/EBPβ promotes transition from proliferation to hypertrophic differentiation of chondrocytes through transactivation of p57. *PLoS One* **4,** e4543 CrossRef Medline
43. Tsuchimochi, K., Otero, M., Dragomir, C. L., Plumb, D. A., Zerbini, L. F., Libermann, T. A., Marcu, K. B., Komiya, S., Ijiri, K., and Goldring, M. B. (2010) GADD45β enhances Col10a1 transcription via the MTK1/MKK3/6/p38 axis and activation of C/EBPβ-TAD4 in terminally differentiating chondrocytes. *J. Biol. Chem.* **285,** 8395–8407 CrossRef Medline
44. Hirata, M., Kugimiya, F., Fukai, A., Saito, T., Yano, F., Ikeda, T., Mabuchi, A., Sapkota, B. R., Akune, T., Nishida, N., Yoshimura, N., Nakagawa, T., Tokunaga, K., Nakamura, K., Chung, U. I., *et al.* (2012) C/EBPβ and RUNX2 cooperate to degrade cartilage with MMP-13 as the target and HIF-2α as the inducer in chondrocytes. *Hum. Mol. Genet.* **21,** 1111–1123 CrossRef Medline
45. Ghosh, H. S., Reizis, B., and Robbins, P. D. (2011) SIRT1 associates with eIF2-α and regulates the cellular stress response. *Sci. Rep.* **1,** 150 CrossRef Medline
46. Sun, T., Li, X., Zhang, P., Chen, W. D., Zhang, H. L., Li, D. D., Deng, R., Qian, X. J., Jiao, L., Ji, J., Li, Y. T., Wu, R. Y., Yu, Y., Feng, G. K., and Zhu, X. F. (2015) Acetylation of Beclin 1 inhibits autophagosome maturation and promotes tumour growth. *Nat. Commun.* **6,** 7215 CrossRef Medline